

Order-parameter profile at long distances in an adsorbed binary liquid mixture near criticality

Mark Schlossman, Xiao-Lun Wu, and Carl Franck

Laboratory of Atomic and Solid State Physics and Materials Science Center, Cornell University, Ithaca, New York 14853

(Received 20 August 1984)

Adsorption of a binary liquid mixture near criticality onto a solid glass substrate can be studied using light reflected off the glass/liquid boundary. Reflectivity data analyzed with a modified Landau-Ginzburg theory using a contact wall interaction are consistent with an exponential decay of the order parameter into the bulk. This analysis provides a measure of h_1 , the effective glass/liquid interaction strength. The reflectivity can also be expressed as an expansion in the moments of the order-parameter profile. For the data presented and an exponential profile the expansion can be truncated at the first-order moment, M_1 . We assume an exponential form of the profile to express the zeroth moment as a function of M_1 . The first moment is fitted as a power law in t , the reduced temperature. Analysis of these preliminary data yields an exponent $p = 0.88 \pm 0.10$ that is consistent with the prediction $p = 2\nu - \beta$ from the scaling law of Fisher and de Gennes.

I. INTRODUCTION

One of the two components of a binary fluid mixture in the vicinity of a wall may be preferentially attracted to the wall. This attraction alters the chemical composition of the liquid near the wall. Long-range composition fluctuations that occur as the binary fluid approaches (from the single phase) its critical demixing point cause the perturbation in the chemical composition due to the wall to extend further from the wall. The chemical composition profile can be expressed in terms of an order parameter $m(z)$, where z is the distance from the wall. The order parameter for our carbon disulfide and nitromethane liquid mixture will be taken as the local chemical concentration (expressed as the volume fraction) of carbon disulfide minus the overall critical concentration of carbon disulfide.

Assuming a contact interaction between the liquid and the wall, the order-parameter profile $m(z)$ is expected to vary as^{1,2}

$$m(z) = C_c (a/z)^{\beta/\nu} \text{ for } a \ll z \ll \xi \text{ or } t = 0 \tag{1}$$

and

$$m(z) = C_\infty e^{-z/\xi} \text{ for } z \gg \xi,$$

where $t = (T - T_c)/T_c$, and T_c is the critical demixing temperature (T and T_c in K), ξ is the bulk correlation length, $\beta/\nu \approx 0.5$ for a three-dimensional binary fluid, a is a molecular size, and C_c and C_∞ are independent of z . Note that the order parameter in the bulk $m(z = \infty)$ is equal to 0 for $t > 0$ (our liquid mixture has an upper critical point).

The exponential decay in (1) at large distances from the perturbing wall is expected generally from theories with short-range wall forces. The existence of long-range wall forces may produce a nonexponential decay at long distances. In particular, long-range van der Waals forces may be important in binary liquids, however, for this paper we will assume that short-range forces determine the behavior of our liquid mixture.

The pure components used for the liquid mixture have

different optical dielectric constants, therefore the composition (or order parameter) profile is manifest as a dielectric constant profile of the liquid mixture near the glass wall (see Fig. 1). The intensity of light reflected off the wall/liquid interface (see Fig. 1) will not be at the Fresnel value predicted for an ideal interface (one with no spatial variation of the dielectric constant except for a discontinuity at the interface), but will indicate the presence of the profile. Theories that relate the order parameter to the reflectivity will be discussed in Sec. III.

The reflectivity can be expressed as an expansion in the moments of the order-parameter profile. An analysis of our data in terms of these moments is presented in Sec. III A. A modified Landau-Ginzburg theory which predicts the profile in (1) can be used to fit the reflectivity. This alternative analysis is presented in Sec. III B. The following section discusses the experiment and the data.

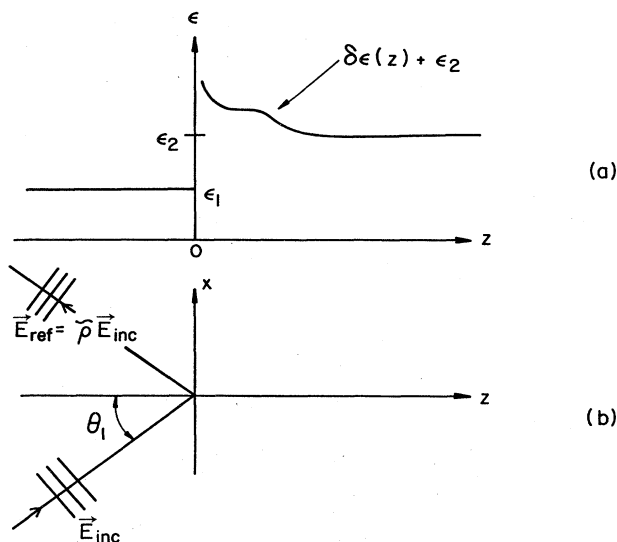


FIG. 1. (a) Dielectric constant as a function of distance. The materials are glass when $z < 0$ and bulk liquid when $z \rightarrow \infty$. (b) Ray diagram for experiment.

II. EXPERIMENT AND DATA

Several experiments have studied order-parameter profiles³⁻⁷ due to adsorption near criticality. Our experiment is similar to that of Franck and Schnatterly,⁴ but with minor modifications to improve the stability of the sample cell and the accuracy of the measurements.

The sample cell is shown in Fig. 2. Details of its construction can be found in Refs. 4 and 8. The glass surface was hydroxylated as described in Ref. 8. This procedure leaves polar hydroxyl (OH) groups on the surface of the glass. We expect these polar groups to preferentially attract the polar nitromethane molecules.^{4,8} The liquid mixture was prepared to within 1% of the critical concentration.⁸ The optical dielectric constant for the glass is $\epsilon_1=2.304$, and the bulk dielectric constant near the critical point is $\epsilon_0=2.202$. The angle of incidence is slightly smaller than the angle of incidence for total internal reflection near the critical point (see the Appendix).

The laser beam reflects off the boundary between the glass prism and the liquid mixture (see Fig. 2). The intensity of reflected light (the reflectivity) is measured as described in Ref. 4. Temperature control and measurement are also described in Ref. 4. The modifications from the experiment of Franck and Schnatterly⁴ allowed us to take data over a wider temperature range in one data run, to reduce the drift of the critical temperature (to 2 mK/24 h) during the data run, and to locate more precisely the bulk critical temperature.

The data for reflectivity of p -polarized light (light with its electric field vector in the plane of incidence) are plotted in Fig. 3. The data in the critical region rise above the bulk background indicating that nitromethane (the upper lighter phase with smaller dielectric constant) is adsorbing onto the surface. The increase in reflectivity as the temperature is increased is evidence of the thermal expansion (which reduces the dielectric constant) of the bulk liquid. The region of reflectivity equal to 1 for $\log_{10}t > -2.3$ is due to total internal reflection. The cooling data are generally slightly higher than the heating data in this region. We suspect that the rounding of the corner at

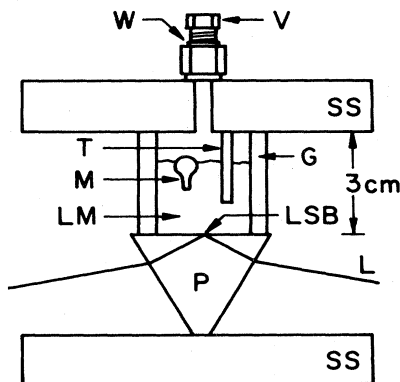


FIG. 2. Horizontal view of sample cell. LSB, liquid/solid boundary investigated; LM, liquid mixture; P , prism; L , HeNe (632.8 nm) laser light beam; T , thermistor probe in thin-walled stainless-steel tube; M , magnetic mixer buoy; SS, stainless-steel disk; G , glass cylinder (indium gaskets on the ends); V , VCR fitting with W , which is a silver-plated stainless-steel washer.

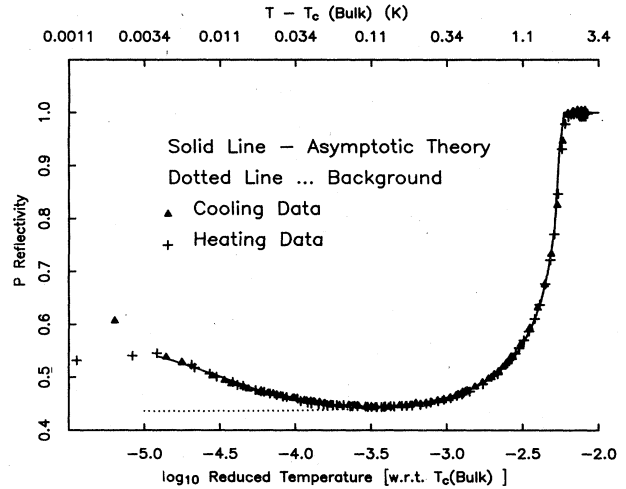


FIG. 3. Measured reflectivity (of p -polarized light) vs temperature. Cooling and heating data are indicated by the symbols. The fit to the asymptotic phenomenological theory (see Sec. III B) is given by the solid line (data used for the fit are in the range $-5.0 < \log_{10}t < -2.3$). The data below $\log_{10}t = -5$ are presumably out of full thermal equilibrium. The background is computed by setting $h_1=0$ (see Sec. III B) and is indicated by the dotted line.

$\log_{10}t = -2.3$ is due to the liquid being slightly out of thermal equilibrium and to averaging over the range of reflection angles that occur because of the finite divergence of the laser beam. These effects will not affect the analyses in this paper. The scatter in the points for $\log_{10}t < -5.0$ presumably occurs because the fluid is not in full thermal equilibrium. The reflectivity contains an experimental error of 0.003, therefore, the cooling and heating curves disagree by more than the experimental error in this region.

The data were taken over a 15-h period while cooling from a high temperature [$T - T_c(\text{bulk}) = 3$ K] to a temperature 0.03 K below the bulk T_c and then while heating over the same temperature range. The temperature was changed by 1 mK/5 min in the critical region ($T - T_c < 0.03$ K) and was measured with an accuracy of 0.5 mK. The T_c drift during the entire data run was approximately 1 mK. Bulk T_c was measured by visually observing swirling of phase separated eddies induced by a mixer in the sample fluid during the cooling and heating temperature scans. The measured bulk T_c is 63.401 ± 0.001 °C. We suspect that, although our calibration is not absolute, this value is significantly higher than the published value^{9(b)} of 61.98 °C because of impurities.

III. ANALYSIS

A. Reflectivity and moments of the order parameter

The moments of the order-parameter profile, M_n , are defined as

$$M_n = \int_0^\infty z^n m(z) dz. \quad (2)$$

As shown in the Appendix the reflectivity can be expressed as a function of these moments. The deviation ΔR of the measured reflectivity R from the Fresnel bulk contribution r^2 can then be written as

$$\begin{aligned}\Delta R_{p,s} &= R_{p,s} - r_{p,s}^2 \\ &= [(\omega/c)^4 (s_{p,s}^2 a_0^2) M_0^2] - (k\xi) [(2\omega^2/c^2) (s_{p,s} r_{p,s} a_0) (M_1/\xi)] \\ &\quad + (k\xi)^2 \{ (\omega/c)^4 (s_{p,s}^2 a_0^2) [(M_1^2 - M_0 M_2)/\xi^2] \} + O((k\xi)^3).\end{aligned}\quad (3)$$

The subscripts refer to polarizations p (in the plane of incidence) and s (out of the plane incidence). Only p -polarized light was used for our experiment. The quantities $r_{p,s}$ and $s_{p,s}$ depend only on bulk parameters and can be written in terms of the dielectric constants of the glass (ϵ_1) and the bulk liquid (ϵ_2), the incident wave vector (k_1), and the z component (perpendicular to the wall) of the transmitted wave vector (k_2) far into the bulk liquid [see Eqs. (A6)–(A8)]. The quantity ω/c is equal to $2\pi/\lambda$, where λ is the light wavelength (632.8 nm). The parameter a_0 is introduced to relate (via the Lorentz-Lorenz relation) the order parameter to the deviation of the dielectric constant from its bulk value [$\epsilon(z=\infty)=\epsilon_2$] as

$$\delta\epsilon(z) = \epsilon(z) - \epsilon(z=\infty) = a_0 m(z). \quad (4)$$

This result is produced by averaging the molecular polarizability of the mixture (see Appendix A in Ref. 8). Assuming no volume change due to mixing and published values for the dielectric constants and densities of the pure liquids,¹⁰ the parameter $a_0=0.77$.

The expansion parameter is $k\xi$, where $k=2k_2$ and ξ is the bulk correlation length $\xi=\xi_0^+ t^{-\nu}$ (the amplitude $\xi_0^+=0.3$ nm and the bulk exponent $\nu=0.63$ are typical experimental values¹¹ for binary liquids). The expansion is satisfactory if the first few terms dominate the others. For our data the parameter $k\xi$ is less than 0.5 for the data in full thermal equilibrium. As explained in the Appendix, k is small because the angle of incidence is close to the critical value for total internal reflection. The terms of order $(k\xi)^2$ will be explicitly shown to be small later in this paper.

In principle, a measurement of the reflectivity of s - and p -polarized light as a function of angle of incidence could yield both M_0 and M_1 [assuming terms of order $(k\xi)^2$ are neglected]. Such an experiment is being developed. In this paper we will extract the first moment from the p -polarized reflectivity data (for fixed angle of incidence and wavelength).

Throughout this paper we will refer to the four terms in the reflectivity equation (3) as the M_0^2 , M_1 , M_1^2 , and M_2 terms [where the last two are both of order $(k\xi)^2$]. Both the M_0^2 and M_1 terms are likely to be important. The M_0^2 term is zeroth order in $k\xi$ and the M_1 term is first order in $k\xi$. The M_1 term cannot be disregarded because it is the lowest order term that can change the sign of ΔR . If the M_1 term dominates, then the sign of ΔR is related to the sign of the surface field h_1 .⁸ The measured reflectivity minus the bulk background could then become negative if the component of higher dielectric constant (carbon disulfide) were adsorbed onto the surface.⁸ As will be shown, the M_1 term dominates near criticality. Modeling M_0 as a function of M_1 will allow the computation of M_1 from the reflectivity.

The small value of $k\xi$ shows that only distances larger than a bulk correlation length are being probed. As previ-

ously mentioned, theories with short-range forces are expected to exhibit an exponential decay of the order parameter for large distances. We will assume the order parameter has the form

$$m(z) = m(z=0, t) e^{-z/\xi}. \quad (5)$$

This profile yields [using Eq. (2)]

$$M_0 = M_1/\xi \quad (6)$$

and

$$M_2 = 2\xi M_1.$$

The $z^{-\beta/\nu}$ aspect of the profile [see Eq. (1)] would yield a relation¹² for M_0 similar to that in Eq. (6). The expansion, however, could not be used for a pure $z^{-\beta/\nu}$ profile because higher moments would diverge.

Values of the temperature-dependent prefactor $m(z=0, t)$ in (5) were computed [using $m(z=0, t) = M_1/\xi^2$] in the calculations to be discussed. The magnitude of the prefactor is small and varies from 0.05 to 0.01 in the critical region (smaller values are nearer T_c), therefore, the perturbation in the bulk liquid produced by the wall is small.

Equation (6) was used in the reflectivity Eq. (3) to compute the value of M_1 from the data shown in Fig. 3. This computation requires the computation of the bulk parameters r_p and s_p given in the Appendix. These were computed by fitting data in the bulk thermal expansion part of the curve to the bulk dielectric constant ($\epsilon_{\text{bulk}}=\epsilon_2$) expressed as

$$\epsilon_{\text{bulk}}^{1/2} = \epsilon_0^{1/2} + Dt + bt^{1-\alpha}, \quad (7)$$

where ϵ_0 , D , and b are constants and $\alpha=0.11$ is the specific heat exponent. The term $bt^{1-\alpha}$ (the dielectric constant bulk anomaly, see Refs. 8 and 10 of Ref. 4) may (if $b>0$) cause the reflectivity to increase in the critical region. Franck and Schnatterly⁴ showed that the bulk anomaly alone cannot explain the observed increase in the reflectivity near the critical point. The critical temperature was fixed at the observed bulk value.

The bulk dielectric constant was fit in the temperature range $-2.9 < \log_{10} t < -2.3$. In this region the term Dt and the term $bt^{1-\alpha}$ show very similar dependence on temperature, thus, over this temperature region a wide range of values for the parameters D and b give a good fit. For simplicity the parameter b was set to zero. The fit then yields $\epsilon_0^{1/2}=1.4841$ and $D=-0.2617$ with a reduced $\chi^2=0.42$ (34 degrees of freedom). The sensitivity of M_1 to variations in the temperature range used for the bulk fit and to inclusion of a nonzero b will be discussed.

The computed value of M_1 and Eq. (6) were then used to compute the contributions of the M_1 , M_0^2 , and M_1^2 terms to ΔR in the reflectivity equation (3) (see Fig. 4). The small M_1^2 term indicates the validity of the expansion in (3) for this temperature range. The expression for M_2

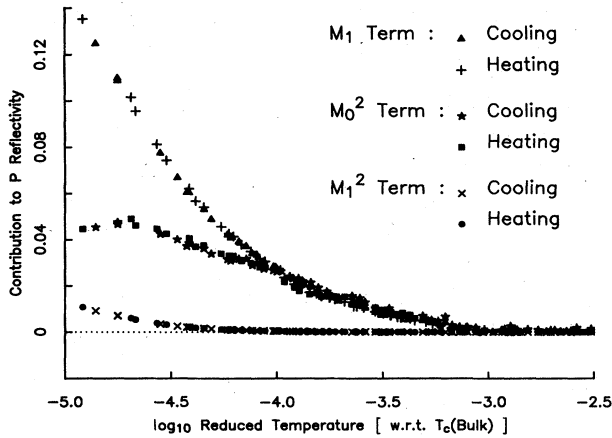


FIG. 4. Values of the individual terms in the expansion ΔR vs temperature. The quantity ΔR is the deviation in the reflectivity from its bulk value (in the absence of surface adsorption). Three of the terms in Eq. (3) were calculated for the cooling and heating data. The M_1^2 term is of order $(k\xi)^2$ and its relative smallness shows that the expansion can be truncated at terms of order $k\xi$.

in terms of M_1 [Eq. (6)] inserted into the term with M_2 in (3) shows that this term is similar in magnitude to the M_1^2 term. For the rest of this paper, unless explicitly stated, terms of order $(k\xi)^2$ will be ignored. Figure 4 shows that the M_1 term dominates near the critical point. Far from the critical point all the terms are small, and the M_0^2 term dominates (not evident from Fig. 4).

In Fig. 5, $\log_{10}(-M_1)$ computed using Eq. (3) without the terms of order $(k\xi)^2$, is plotted versus $\log_{10}t$. The region $\log_{10}t > -3.2$ is further than 0.2 K from bulk T_c and the scatter occurs in this region because the reflectivity here is primarily a bulk effect. The data exhibit a linear region for $-4.6 < \log_{10}t < -4.0$ (equivalently, 63.409°C

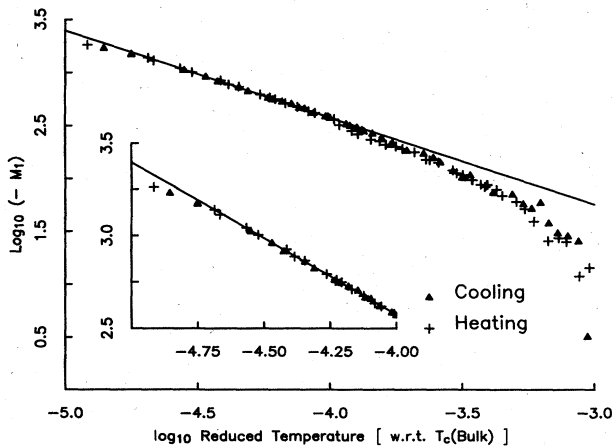


FIG. 5. Logarithmic plots of the magnitude of the first profile moment $|M_1|$ vs the reduced temperature t . Cooling and heating data are indicated by the symbols. The line is a power-law fit to the region $-4.6 < \log_{10}t < -4.0$. The inset is a detail of the fit.

TABLE I. The first moment fitted as a power law in the reduced temperature. The functional relationship is $-M_1 = ct^{-p}$.

Range of $\log_{10}t$		c	p	rms deviation
Minimum	Maximum			
-4.6	-4.0	0.19	0.82	5.5×10^{-3}
-4.6	-3.5	0.065	0.93	2.2×10^{-2}
-5.0	-3.5	0.096	0.89	3.0×10^{-2}
-5.0	-3.75	0.15	0.85	2.4×10^{-2}
-5.0	-4.0	0.28	0.78	1.1×10^{-2}

$< T < 63.435^\circ\text{C}$). A linear fit for this temperature range is displayed in Fig. 5 and a closer view in the inset of that figure. This fit corresponds to $-M_1 = ct^{-p}$, where $c=0.19$ and $p=0.82$ (errors to be discussed). This fit includes 29 points (from the heating and cooling curves). For comparison, fits over slightly different ranges were calculated though the quality of the fits was lower (see Table I). Although Table I indicates that the fit parameters are sensitive to the temperature range of data used for the fit, the region that gives the best fit is unambiguous. The same fits were performed for M_1 calculated from all the terms in Eq. (3). The results were almost exactly the same as those listed in Table I. The temperature range for the best fit was also the same. Another aspect of the analysis that can introduce error into the calculation of the power-law exponent p and the constant prefactor c is the temperature range used for the fit to the bulk thermal expansion part of the data. Doubling the number of points used for the bulk fit [still with $b=0$; see Eq. (7)] affects the resultant fit for M_1 only slightly. The most significant error in the fit is due to our imprecise knowledge of the bulk dielectric constant anomaly. The effect of a nonzero b can be gauged by using the parameters from the fit to the asymptotic theory presented in Table II (to be discussed later in this paper) to compute M_1 . The value of b depends on the particular theory we used. The power-law fit of M_1 as a function of t yielded $c=0.044$ and $p=0.95$ (rms deviation of 7.8×10^{-3} ; see Table I for comparison). This fit can be used only as a qualitative guide to the error introduced by the uncertainty in the bulk anomaly. Including all errors mentioned an estimate for p and c is $p=0.88 \pm 0.10$ and $c=0.15 \pm 0.10$.

A theoretical prediction can be made for the temperature dependence of the first moment of the order parameter. Fisher and de Gennes¹ presented the following scaling law for $m(z)$ subject to a contact wall interaction of strength h_1 :

$$m(z) = t^\beta Y(z/\xi; h_1 t^{-\Delta_1}), \quad (8)$$

where Y is a scaling function. Using the definition of M_1 and the scaling law (8)

$$\begin{aligned} M_1 &= t^{\beta-2\nu\xi^2} \int_0^\infty y Y(y; h_1 t^{-\Delta_1}) dy \\ &\equiv t^{\beta-2\nu\xi^2} I \quad \text{with } y = z/\xi. \end{aligned} \quad (9)$$

As $h_1 \rightarrow \infty$, $m(z)$ must remain finite, therefore, we assume $Y(y, x \rightarrow \infty) = Y_\infty(y)$ (this limit is also evident from a classical calculation¹³ of the scaling function for M_1).

More generally we postulate that for the particular value of h_1 and range of t in our experiment, the scaling function loses its h_1 dependence. This assertion warrants further experimental investigation. If $t \rightarrow 0$, the integral I will then be independent of t . Equation (9) then predicts

$$M_1 \sim t^{-(2\nu-\beta)}. \quad (10)$$

B. Modified Landau-Ginzburg theory

Another method of analysis is to fit to the expected profiles in Eq. (1). The limits in (1) for $t > 0$ are contained in the solution to the following modified Landau-Ginzburg free-energy density:^{15,16(a),2}

$$G(z) = (k_B T_c / a^3) \left[(a^2/2) \left(\frac{\partial m}{\partial z} \right)^2 \pm (a^2/2) [m^2 / (\xi^\pm)^2] + (v_0/6) m^6 \right] - h_1 m \delta(z), \quad (11)$$

which assumes the validity of the approximations $2\beta = \nu$ and $\eta = 0$. In this phenomenological theory the contact interaction h_1 at the wall results in a preferential attraction of one of the fluid components. Our definition of the order parameter implies that $h_1 < 0$ favors adsorption of the polar nitromethane to the polar wall. As mentioned before, a is a molecular size. The plus and minus signs on the m^2 term and in the superscript of the correlation length, $\xi^\pm \sim \xi_0^\pm t^{-\nu}$, correspond to, respectively, $t > 0$ and $t < 0$. The constant v_0 is evaluated in the homogeneous system with $h_1 = 0$ when $t < 0$. For this evaluation we assumed that $\xi_0^+ = \xi_0^-$. Theory and experiments¹⁷ on other liquid mixtures indicate that $\xi_0^+ = 2\xi_0^-$. The constant v_0 is evaluated in terms of the order-parameter amplitude⁹ B and the correlation length amplitude ξ_0^+ ; $v_0 = 16a^2/[B^4(\xi_0^+)^2]$. In this free-energy density a surface-coupling term proportional to m^2 is neglected.²

Free-energy densities with an m^6 term are usually used to describe tricritical behavior¹⁶ and contain singularities at $t = 0$ for many compositions of the mixture. These singularities are not appropriate for describing the critical demixing transition in a binary liquid, however, this free-energy density was introduced^{15,2} as an *ad hoc* adjustment of the m^4 classical theory which has critical exponents that more closely approximate the nonclassical values. We will use the m^6 theory for $t > 0$ to avoid the unwanted singularities as much as possible.

Although the theory is pathological, it can be a useful tool. In particular it will show that within the context of a theory with a contact wall/liquid interaction our data exhibit only exponential decay of the order parameter. This will reinforce our assumption of exponential decay used for the analysis in terms of moments. In addition, values for the bulk dielectric constant will be extracted. These values were already used to estimate errors in the moments analysis. Finally, by fitting h_1 to our experiment we will find the effective surface field strength.

The total free energy $F = \int_0^\infty d^3x G(z)$ is minimized as usual, yielding (for $t > 0$)

$$\frac{\partial^2 m}{\partial z^2} - m / (\xi^+)^2 - (v_0/a^2) m^5 = 0 \quad (12)$$

and

The approximate experimental values¹⁴ $\beta = 0.33$ and $\nu = 0.63$ yield $p = 2\nu - \beta = 0.93$. This value is within the experimental errors of the measurement. Equation (10), however, may not be appropriate because the data may not be in the asymptotic scaling region $t \rightarrow 0$.

$$\left. \frac{\partial m}{\partial z} \right|_{z=0} = -h_1 a / k_B T_c.$$

These have the solution

$$m(z) = \frac{m(0) 2^{1/2} e^{z/\xi} [1 + (1+w)^{1/2}]^{1/2}}{\{[1 + (1+w)^{1/2}]^2 e^{4z/\xi} - w\}^{1/2}} \quad (13)$$

with

$$m(0) = (v^{1/2} \{[(1+q)^{1/2} + 1]^{1/3} - [(1+q)^{1/2} - 1]^{1/3}\})^{1/2} \text{sgn}(h_1)$$

and

$$w = \frac{16}{3} [m(0)/B]^4 t^{-2\nu},$$

$$v = \left(\frac{3}{32}\right)^{1/3} [B^2 (h_1 a \xi_0^+ / k_B T_c)]^{2/3},$$

$$q = (t^{6\nu}/36) [B / (h_1 a \xi_0^+ / k_B T_c)]^4,$$

where $B = 1.63$ is the published order-parameter amplitude.^{9(b)} In the limit $t \rightarrow 0$ the variable q vanishes and, therefore, $m(0)$ is independent of t . This implies that $w \rightarrow \infty$. Fixing z and taking $z \ll \xi$, we find this solution reproduces the power-law behavior [Eq. (1)] deduced from scaling arguments¹ and also from renormalization-group calculations.¹⁸ In the limit of $z \gg \xi$, the solution (13) reduces to the asymptotic solution

$$m(z) \approx m(0) \frac{2^{1/2}}{[1 + (1+w)^{1/2}]^{1/2}} e^{-z/\xi}. \quad (14)$$

Note that as $t \rightarrow 0$, w vanishes and (14) reduces to $m(z) \approx m(0) e^{-z/\xi}$ as expected for phenomenological theories with a short-range wall interaction.

The fitting procedure consists of three stages: (i) applying the Lorentz-Lorenz relation to the solution to obtain the dielectric constant profile [see Eq. (4)], (ii) using our first-order Born approximation optical theory (see Ref. 19 and the Appendix) to deduce the reflectivity from the dielectric constant profile [Eq. (7) provides ϵ_{bulk} in terms of the parameters $\epsilon_0^{1/2}$, D , and b], and (iii) fitting²⁰ the measured reflectivity to the predicted reflectivity.

The parameter ξ_0^+ was fixed at $\xi_0^+ = 0.3$ nm (a typical value¹¹ for binary liquids), and the parameters $\epsilon_0^{1/2}$, D , b ,

TABLE II. Parameters for the fits to the phenomenological theories.

Quantity	Asymptotic theory		Full theory	
	Value	Standard deviation	Value	Standard deviation
χ_{red}^2	0.69		0.69	
T_c (°C)	63.3897	3×10^{-4}	63.3892	4×10^{-4}
h_1^{red}	-1.2×10^{-4}	1.2×10^{-5}	-1.3×10^{-4}	5×10^{-6}
b	0.2014	4×10^{-3}	0.1918	4×10^{-3}
$\epsilon_0^{1/2}$	1.4839	4×10^{-6}	1.4839	4×10^{-6}
D	-0.6003	7×10^{-3}	-0.5845	7×10^{-3}

$h_1 a / k_B T_c$, and T_c were fitted to the data. Fits were made to the full theory and its asymptotic ($z \gg \xi$) limit.

The fit to the asymptotic theory is plotted with the data in Fig. 3. The first feature to note is the good agreement of the fit in the region $-5.0 < \log_{10} t < -2.3$. This shows that the data in thermal equilibrium are well fitted. The fitting parameters are listed in Table II. The value $h_1^{\text{red}} = h_1 a \xi_0^+ / k_B T_c$ listed in the table is a dimensionless version²¹ of h_1 where we let $a = \xi_0^+$. This reduced surface field expresses the ratio of surface energy over a unit area of intermolecular spacing to the thermal bulk energy at $t=0$. Its small value indicates that the solid/liquid interaction is weak. The sign of h_1^{red} indicates that nitromethane (the more polar molecule) is preferentially adsorbing onto the hydroxylated glass surface (see Ref. 8 for a discussion of the importance of surface chemistry in tuning the value of the surface field).

As previously mentioned, both the dielectric constant bulk anomaly [if $b > 0$; see Eq. (7)] and critical adsorption may cause the reflectivity in the critical region to increase. Without an independent experimental measurement of the bulk anomaly the dependence of the fits on the parameters b and h_1 must be treated with care. A standard deviation for the estimates for h_1 which accounts for cross correlations between h_1 and the other fitting parameters in the asymptotic fit was computed by fixing h_1 at various values, fitting to the other variables and plotting the reduced χ^2 vs h_1 . All the other standard deviations quoted were taken from the diagonal elements of the error matrix of the fitting routine²⁰ and may be underestimated.

Franck and Schnatterly⁴ showed that the increase in the reflectivity near T_c due to the bulk anomaly is expected to be small compared with the reflectivity increase due to the critical adsorption. Although small, the bulk anomaly contributes to the precision of the fit. An asymptotic fit with $b=0$ imposed yielded a reduced $\chi^2=1.3$. This is almost twice the value for the reduced χ^2 found when using b as a fit parameter (see Table II) and indicates a significant difference in a fit with 129 degrees of freedom (134 data points minus 5 fit parameters).

A more detailed graph of the critical region is shown in Fig. 6. Fits to both the full phenomenological solution (13) and its asymptotic version (14) are displayed. The fits are indistinguishable on this scale and have a slightly different curvature than the data. Near the critical point the data seems to diverge more strongly than the fit. This may account for the difference $T_c(\text{bulk}) - T_c(\text{fit}) = 11$

mK. The most important feature (of Fig. 6) is the indication that the two different fits are equally valid for these data. Within the context of the contact theory, the data indicate that only the exponential aspect of the order parameter profile is being probed. As has been shown, this result is expected because the experiment examined only behavior at distances large compared with the bulk correlation length.

An exponential profile results even when the m^6 term in Eq. (11) is ignored. The data, therefore, do not provide evidence for the power-law behavior in Eq. (1).

Our observations of the reflectivity of the interface between a critical binary liquid mixture and a selectively adsorbing wall are consistent with the exponential order-parameter profile predicted for large distances by theories with short-range wall forces. The consistency of our observations with other theories such as those with long-range wall forces is an open question. An analysis of the first moment of the order-parameter profile as a function of reduced temperature t shows a simple power-law region ($-M_1 = ct^{-p}$) over slightly less than a decade in t . The scaling law of Fisher and de Gennes¹ provided an estimate

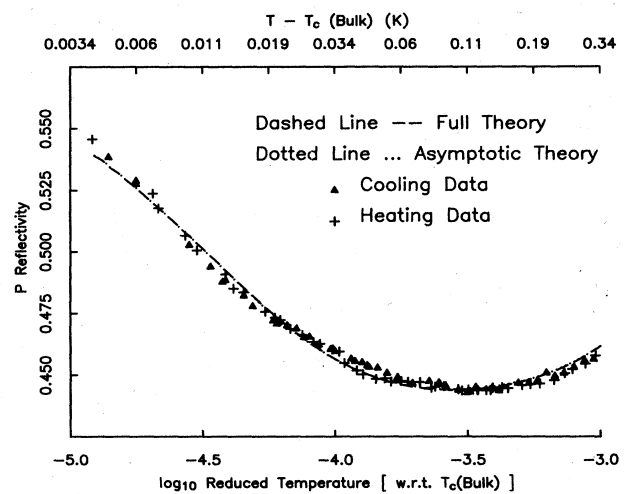


FIG. 6. Reflectivity (of p -polarized light) vs temperature in the critical region. Cooling and heating data are indicated by the symbols. The fits to the asymptotic and the full phenomenological theories are given by the lines and are indistinguishable on this scale. The data used for the fit are in the range $-5.0 < \log_{10} t < -2.3$.

for p that lies within the experimental error of the measurement. This estimate assumes that these data are in the asymptotic scaling region. A phenomenological theory is in good agreement with the reflectivity data and indicates that exponential long-distance behavior dominates in our experiment. We find that the adsorption at long distances is a weak effect in the following two senses: The moments analysis yields a small amplitude and the fit to the phenomenological theory produces a small value for the effective surface field. Further work will emphasize model-independent analysis of optical data to better understand the structure of a critically adsorbed liquid.

ACKNOWLEDGMENTS

We appreciate the assistance of Professor P. G. de Gennes, Professor B. Widom, Professor W. W. Webb, Dr. H. van Doremalen, Dr. V. Privman, Dr. M. Robert, Dr. S. Leibler, and Mr. M. Hirsch. We particularly thank Professor M. E. Fisher and Dr. M. B. Schneider for their careful reading and many suggestions concerning the physics and clarity of this manuscript. One of us (M.S.) wishes to thank IBM and Exxon for funding through an industrial liaison program with the Cornell University Department of Physics. One of us (C.F.) wishes to thank the organizers of the Les Houches School of Physics in France for their hospitality. The support of the National Science Foundation through the Materials Science Center of Cornell University is gratefully acknowledged.

APPENDIX: OPTICAL THEORY AND MOMENTS OF THE ORDER PARAMETER

The half-space Fourier transform of the dielectric function profile, $\delta\epsilon(z)$, where $\delta\epsilon(z) = \epsilon(z) - \epsilon(z = \infty)$, arises naturally as the crucial quantity for the reflectivity in the first-order Born-approximation optical theory,¹⁹

$$\delta\tilde{\epsilon}(k) = \int_0^\infty e^{ikz} \delta\epsilon(z) dz, \quad (\text{A1})$$

where k is twice the z component of the transmitted wave vector far into the bulk liquid and is given by

$$k = 2\epsilon_2^{1/2}(\omega/c)\cos\theta_2 \quad (\text{A2})$$

with $\epsilon_2 = \epsilon_{\text{bulk}}$ and $\omega/c = 2\pi/\lambda$. The wavelength in vacuum is λ and θ_2 is the angle of transmission in the absence of a perturbation, so

$$\cos\theta_2 = [1 - (\epsilon_1/\epsilon_2)\sin^2\theta_1]^{1/2}, \quad (\text{A3})$$

where θ_1 is the angle of reflection (see Fig. 1).

The complex reflectivity amplitude $\tilde{\rho}$ is defined in terms of the reflected and incident electric field vectors (see Fig. 1) by

$$E_{p,s}^{\text{ref}} = \tilde{\rho}_{p,s} E_{p,s}^{\text{inc}} \quad (\text{A4})$$

The subscripts refer to polarizations p (in the plane of in-

cidence) and s (out of the plane of incidence). The optical theory¹⁹ shows that the amplitude can be written as

$$\tilde{\rho}_{p,s} = r_{p,s} + i(\omega/c)^2 s_{p,s} \delta\tilde{\epsilon}(k). \quad (\text{A5})$$

The quantities $r_{p,s}$ and $s_{p,s}$ depend only on the bulk parameters and r is the Fresnel reflection coefficient. For p polarization the expressions are

$$r_p = \frac{\epsilon_2 k_1 - \epsilon_1 k_2}{\epsilon_2 k_1 + \epsilon_1 k_2} \quad (\text{A6})$$

and

$$s_p = \frac{2\epsilon_1 \epsilon_2 k_1 (1 - 2\cos^2\theta_2)}{(\epsilon_2 k_1 + \epsilon_1 k_2)^2},$$

while for s polarization the expressions are

$$r_s = \frac{k_1 - k_2}{k_1 + k_2} \quad (\text{A7})$$

and

$$s_s = \frac{2k_1}{(k_1 + k_2)^2},$$

where

$$k_1 = \epsilon_1^{1/2}(\omega/c)\cos\theta_1 \quad (\text{A8})$$

and $k_2 = k/2$, while ϵ_1 is the dielectric constant for the glass wall (see Fig. 1). The reflectivity is given by

$$R_{p,s} = |\tilde{\rho}_{p,s}|^2. \quad (\text{A9})$$

The reflectivity experiment was performed with an angle of incidence ($\theta_1 = 77.6$) close to the critical angle ($\theta_c = 77.85$ near T_c) for total internal reflection. Close to total internal reflection k is small [see Eqs. (A2) and (A3)]. Near the critical temperature $k = 6 \times 10^{-3} \text{ nm}^{-1}$. The Fourier transform can be expanded in powers of k with coefficients containing moments of the dielectric function profile (similar to Ref. 12). Using the relationship in (6), Eq. (A1) can be written as

$$\tilde{m}(k) = (1/a_0)\delta\tilde{\epsilon}(k) = \sum_{n=0}^{\infty} M_n (ik)^n / n!, \quad (\text{A10a})$$

where

$$M_n = \int_0^\infty z^n m(z) dz. \quad (\text{A10b})$$

Equation (A10a) can be conveniently rewritten as

$$\tilde{m}(k) = \sum_{n=0}^{\infty} (M_n / \xi^n) (ik\xi)^n / n! \quad (\text{A11})$$

This expansion will converge for an exponential profile, but for other profiles it may not. The substitution of the bulk correlation length ξ is conventional and provides a convenient dimensionless expansion parameter, $k\xi$. The correlation length ξ is taken from typical experimental results.¹¹ Approximating $m(k)$ in terms of the three lowest moments and substituting into Eqs. (A5) and (A10) the deviation ΔR in Eq. (3) is derived.

- ¹M. E. Fisher and P. G. de Gennes, C. R. Acad. Sci. Ser. B **287**, 207 (1978).
- ²L. Peliti and S. Leibler, J. Phys. C **16**, 2635 (1983).
- ³D. Beaglehole, J. Chem. Phys. **73**, 3366 (1980).
- ⁴Carl Franck and S. E. Schnatterly, Phys. Rev. Lett. **48**, 763 (1982).
- ⁵D. Beysens and S. Leibler, J. Phys. (Paris) Lett. **43**, L-13 (1982).
- ⁶Barbara Heidel and Gerhard H. Findenegg (unpublished).
- ⁷P. S. Pershan and J. Als-Nielsen, Phys. Rev. Lett. **52**, 759 (1984).
- ⁸Janet Dixon, Mark Schlossman, Xiao-lun Wu, and Carl Franck, Phys. Rev. B **31**, 1509 (1985).
- ⁹(a) Using the definition of the order parameter $m = \phi - \phi_c$, where ϕ is the concentration of carbon disulfide, approximate (for $T < T_c$) $m = (\Delta\phi)/2$, where $\Delta\phi$ is the difference between the concentration of CS₂ in one phase and the concentration of CS₂ in the other phase. We then use $\Delta\phi = Bt^\beta$. (b) E. S. R. Gopal, R. Ramachandra, P. Chandra Sekhar, K. Govindarajan, and S. V. Subramanyam, Phys. Rev. Lett. **32**, 284 (1974).
- ¹⁰S. H. Maron and C. F. Prutton, *Principles of Physical Chemistry*, 4th ed. (Macmillan, New York, 1968), p. 693; we used indices for 20°C from *CRC Handbook of Chemistry and Physics*, 60th ed., edited by Robert C. Weast (Chemical Rubber Company, Boca Raton, Florida, 1980); J. R. Partington, *An Advanced Treatise on Physical Chemistry* (Longmans, London, 1953), Vol. 4.
- ¹¹M. A. Anisimov, Usp. Fiz. Nauk. **114**, 249 (1974) [Sov. Phys.—Usp. **17**, 722 (1975)]
- ¹²J. C. Charmet and P. G. de Gennes, J. Opt. Soc. Am. **73**, 1777 (1983).
- ¹³Carl Franck (unpublished).
- ¹⁴D. Beysens, in *Phase Transitions, Status of the Experimental and Theoretical Situation*, edited by M. Levy, S. C. le Guillou, and J. Zinn-Justin (Plenum, New York, 1981), p. 25.
- ¹⁵P. G. de Gennes, C. R. Acad. Sc. Ser. B **292**, 701 (1981); P. G. de Gennes (private communication).
- ¹⁶(a) B. Widom, J. Chem. Phys. **67**, 872 (1977); (b) R. B. Griffiths, J. Chem. Phys. **60**, 195 (1974).
- ¹⁷D. Beysens, A. Bourgou, and P. Calmettes, Phys. Rev. A **26**, 3589 (1982).
- ¹⁸J. Rudnick and D. Jasnow, Phys. Rev. Lett. **49**, 1595 (1982); E. Brezin and S. Leibler, Phys. Rev. B **27**, 594 (1983).
- ¹⁹Carl Franck and V. Celli (unpublished). The approach used is similar to that of Ref. 12. In our case, light is incident from the substrate instead of the liquid side (as in Ref. 12).
- ²⁰The fits to the theory used CURFIT from Philip R. Bevington, *Data Reduction and Error Analysis for the Physical Sciences* (McGraw-Hill, New York, 1969), p. 237.
- ²¹R. Pandit and M. Wortis, Phys. Rev. B **25**, 3226 (1982).